PROCEEDINGS OF SCIENCE

Probing for light new particles with the LUXE experiment

Shan Huang[a,*] **for the LUXE Collaboration**

[a] *Instituto de Física Corpuscular (IFIC), CSIC–UV, 46980 Paterna, Valencia, Spain*

E-mail: shan.huang@ific.uv.es

The proposed LUXE experiment (*Laser und XFEL Experiment*) at DESY, Hamburg, using the electron beam from the European XFEL, aims to probe QED in the non-perturbative regime created in collisions between high-intensity laser pulses and high-energy electron or photon beams. This setup also provides a unique opportunity to probe physics beyond the standard model. In this talk we show that by leveraging the large photon flux generated at LUXE, one can probe axion-like-particles (ALPs) up to a mass of 350 MeV and with photon coupling of 3×10^{-6} GeV^{-1}. This reach is comparable to the background-free projection from NA62. In addition, we will discuss the ongoing optimisation of the experimental setup for the ALP search.

The European Physical Society Conference on High Energy Physics (EPS-HEP 2025)
7-11 July 2025
Marseille, France

*Speaker

 ISSN 1824-8039. Published by SISSA Medialab.

PoS(EPS-HEP2025)431

1. Introduction

The LUXE experiment [1, 2] aims to explore the uncharted regime of strong-field quantum electrodynamics (SFQED) by measuring the collisions between high-energy leptons, extracted from the 16.5 GeV electron beam at the European XFEL via the ELBEX project [3], and a highly intense laser delivering peak powers between 10 to 350 TW. The types of lepton, either electron or photon, correspond to LUXE e-laser and γ-laser running modes. Its detection systems for electrons, positrons, and photons are designed to measure the particles produced at the main interaction point (IP) and to observe the phenomena including nonlinear Compton scattering and nonlinear Breit–Wheeler pair production. The extracted leptons will recur every 0.1 s (10 Hz), while the laser will run at 1 Hz. Over one year of data taking, around 10^7 bunches crossing (BXs) will be collected, each one contains 1.5×10^9 primary electrons extracted via ELBEX.

In the LUXE e-laser mode, the laser beam functions as an "optical dump" converting the primary electrons into high-flux GeV photons via the nonlinear Compton scattering. These Compton photons propagate freely through the laser and end up at a downstream photon dump made of thick high-Z materials. This tightly collimated and highly intense GeV photon beam is unparalleled to any existing photon facility worldwide, and provides a unique opportunity to search for beyond-the-Standard-Model (BSM) particles at LUXE in a beam dump experiment. While most Compton photons are absorbed in the downstream beam dump, a portion of them may convert to the BSM particles X via the Primakoff process, as predicted for ALPs and other models. These feebly interacting particles traverse the dump and decay downstream back into two photons as $\gamma\gamma \to X \to \gamma\gamma$, leading to a characteristic diphoton signal in the detector. The feasibility and projected sensitivity of this concept has been published in the LUXE New Physics at Optical Dump (LUXE-NPOD) phenomenological study [4], The present article summarizes the current status of LUXE-NPOD, includes optimization and validation of the sensitivity with more realistic experimental designs, a more detailed background estimate, and a proof-of-the-concept reconstruction with an off-the-shelf detector. Further details of this study have also been submitted [5]. LUXE aims to start the installation in 2029, and take data with a minimal detector configuration around 2030.

2. Sensitivity

The experimental scheme of LUXE-NPOD is shown in Fig. 1. The projected sensitivity is evaluated using a sequence of simulations. At the LUXE IP, QED phenomena including the

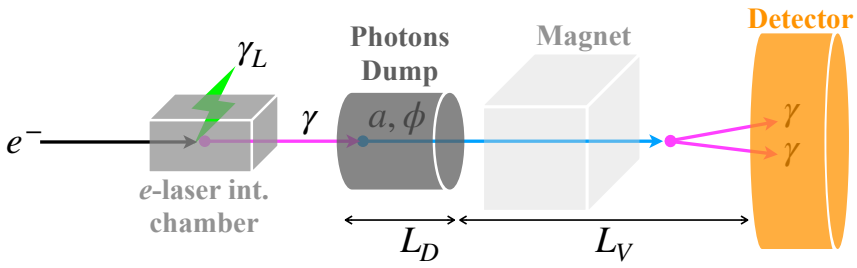

Figure 1: A schematic representation showing the detection of scalar particle a or psudoscalar particle ϕ. Adapted from the LUXE-NPOD proposal [4].

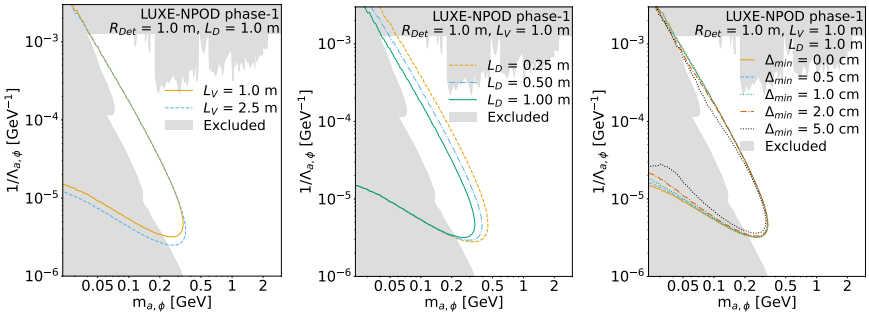

Figure 2: LUXE-NPOD sensitivity scans in ALP phase space of coupling coefficient $1/\Lambda$ and mass m over decay volumes, dump lengths, and separation powers [5].

nonlinear Compton scattering are simulated with Ptarmigan [6], which provides the distribution of the Compton photons in position-momentum phase space. This information is then propagated (1) to MadGraph5 for the interaction between photons and ALPs of mass between 0.01 to 1 GeV, and also (2) to Geant4 for background study in Sec. 3. Three laser configurations are considered with their powers of 10 TW (phase 0.10), 40 TW (phase 0.40), and 350 TW (phase 1).

To maximize the signal efficiency, we study the sensitivity projections when varying the dump length L_D, decay volume L_V, detector radius $R_{\rm Det}$, and detector diphoton separation power $\Delta_{\rm min}$. An energy threshold of $E_{\rm kin} > 0.5\,$GeV is used for the detector. The results are presented in Fig. 2. Extending the decay volume enhances the reach in the low-mass, weak-coupling region by favouring long-lived ALPs, while shortening the dump benefits the high-mass, strong-coupling region where the ALPs are shorter lived. However, a shorter dump may increase the risk of leakage, and the total length $L_D + L_V$ is limited by the available detector radius and size of the experimental hall. Taking $L_D = L_V = 1\,$m, dump radius $R_D = 0.5\,$m, and $R_{\rm Det} = 1\,$m, we find that detectors able to resolve close-by diphoton with 2-cm distance at their entrance can provide sufficient sensitivity coverage.

3. Background

The Geant4 background simulation has been updated with the full-apparatus LUXE geometry. It provides a more reliable estimate that accounts for backscattering from other apparatus and the experimental hall structures. The simulation is used to optimize the photon dump design, including its length L_D, radius R_D, and material composition. A dummy detector with $R_{\rm Det} = 1\,$m is used and the decay volume is set as 2.5 m. Two dominant background sources are identified as neutrons and photons. Other long-lived particles such as pions, protons, muons, and electrons are also considered, but contribute less due to their lower energies and rates. Three categories of dump designs are studied: purely made of tungsten, with L_D up to 100 cm and R_D up to 30 cm; purely made of lead, with $L_D = 100\,$cm, $R_D = 40\,$cm; and a bimetallic dump made of a hollow lead cylinder and a tungsten core, specifically, $L_D = 100\,$cm, $R_D(\mathrm{W}) = 20\,$cm, and $R_D(\mathrm{Pb}) = 50\,$cm.

For phase-0 lasers, the smallest tungsten dump design in the simulations ($L_D = 25\,$cm, $R_D = 10\,$cm) is sufficient to reach a background-free data taking. For phase-1, however, a larger dump is required to suppress the increased leakage (mainly through the sides) and multiple scattering due to a higher Compton photon flux. A coarse scan of 0.5 BX for each dump design shows that

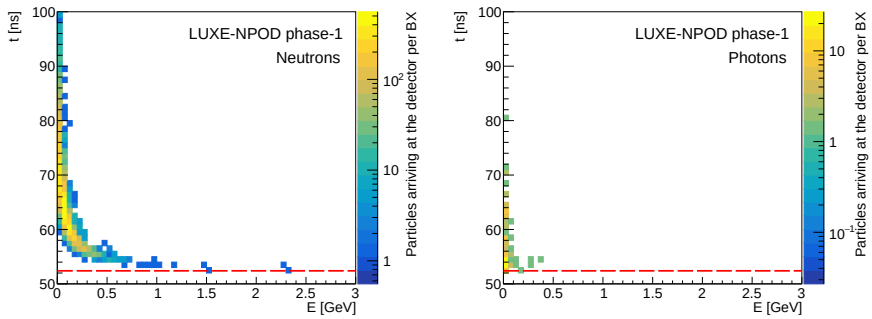

Figure 3: Time of arrival at the detector of (left) background photons and (right) neutrons for the bimetallic dump. The timepoint $t = 0$ is set at the moment of electron-laser collision at the main interaction point of LUXE. The signal photons arrive at the detector at $t = 52.4$ ns, marked by a dashed line [5].

both the largest tungsten dump ($L_D = 100$ cm, $R_D = 30$ cm) and the bimetallic dump reduce above-threshold ($E_{\text{kin}} > 0.5$ GeV) background neutrons to fewer than 10^2 per BX. Note that the bimetallic dump costs less than the 30-cm radius tungsten dump. A pure lead dump lacks comparable stopping power. A detailed 10-BX simulation for the bimetallic design (Figs. 3) shows sub-1.5 GeV neutrons arriving ≥ 1 ns later than the signal photons, enabling timing-based rejection with $\lesssim 1$ ns resolution. Above-threshold charged backgrounds are counted 23 per BX, factor of three fewer than neutrons. Side leakage motivated the use of a larger-radius dump inside concrete; the chosen W+Pb design retains tungsten-like stopping power with lower cost and easier handling. Combined with detector timing and PID, this configuration renders the phase-1 search effectively background free. Additionally, any detector that has a cross section smaller than 1 m would further reduce background. We also explored a magnetized dump but did not find a significant suppression gain.

4. Detector

The NPOD detector must maintain high signal efficiency while rejecting residual backgrounds. In terms of acceptance, it should be large enough to sufficiently cover the phase space, and small enough to avoid off-axis background. The simulation in Sec. 2 shows that a detector with radius of a few tens of centimeters should suffice because the ALPs are produced relativistically and the signal diphotons remain near the axis. To reconstruct the diphoton final state, the detector must measure photon energies, opening angle, and entry point positions in order to infer the decay z-vertex and resolve close-by showers. Hence, we use a sandwich silicon-tungsten sampling calorimeter LUXE ECAL-NPOD. It is based on a prototype of the CALICE/DRD-Calo SiW-ECAL, which also serves as ECAL-E in the LUXE γ-laser mode. (Relocation between modes is under study.) The prototype has an overall size $36 \times 18 \times 22.5$ cm^3, placed on-axis downstream of the photon dump. It consists of 15 layers of 4.2 mm W and 0.5 mm Si, with 64×32 readout pads per layer. Particle interactions with the standalone detector are simulated with DD4hep for single photons, for photon pairs, and for single pions, neutrons, and protons with energies of 0.5 to 3.5 GeV. The simulation data are digitized and analyzed in the Marlin framework; the code is released at an open-source repository [7].

Reconstruction uses nearest-neighbour clustering, straight-line axis fits with cylindrical re-clustering for positions and angles, and a three-class boosted decision tree trained on shower-shape

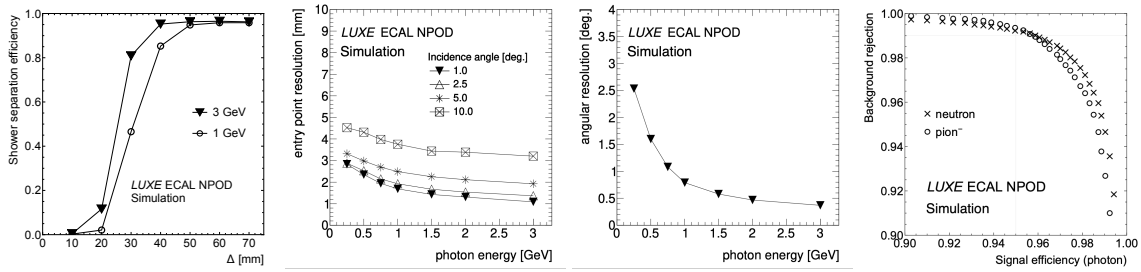

Figure 4: Detector performance summary (left to right): diphoton separation efficiency vs. entry-point distance Δ, entry-point resolution, angular resolution, and neutron/pion rejection vs. photon efficiency [5].

variables to distinguish photons, neutrons, and charged pions. The intrinsic energy resolution obtained from simulation is $\sigma_E/E = (19.8 \pm 0.4)\%/\sqrt{E/\text{GeV}} \oplus (4.9 \pm 0.3)\%$, where E is the photon energy. Photon-pair scans with separations of 10 to 100 mm are used to determine the separation efficiency, requiring at least two clusters with the energy ratio of two leading ones $E_1/E_2 < 2$. Hits outside a cylinder that contains 90% of cluster hits are removed to improve the straight-line fit. Fig. 4 shows full diphoton separation for $\Delta \gtrsim 40$ to 50 mm, position resolution of 1 to 3 mm for $< 5°$ impact angle, angular resolution below 1° above 1 GeV and better than 2° near 0.5 GeV, and BDT rejection of $\sim 99\%$ of neutron/pion backgrounds at $\gtrsim 95\%$ photon efficiency.

5. Conclusion

This article summarizes the recent optimization and validation of the LUXE-NPOD proposal. Its updated reach projection is illustrated in Fig. 5 based on more realistic assumptions and more detailed simulations for geometrical parameters, dump design, and detector performance. In phase-

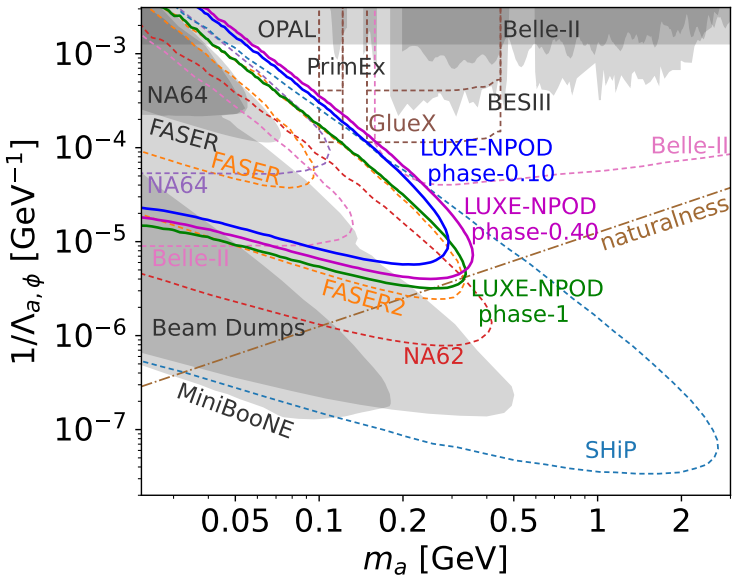

Figure 5: LUXE-NPOD sensitivity with existing bounds (gray regions) and future projects (dashed) [5].

0, a short tungsten dump will be used, allowing exploration to the previously uncharted region in $35\,\text{MeV} \lesssim m_X \lesssim 350\,\text{MeV}$ and $1/\Lambda \lesssim 6 \times 10^6\,\text{GeV}^{-1}$. And the dump will be reconfigured to a bimetallic version for phase-1, shifting the sensitivity towards lighter ALPs in $27\,\text{MeV} \lesssim m_X \lesssim 330\,\text{MeV}$ and $1/\Lambda \lesssim 4 \times 10^6\,\text{GeV}^{-1}$. This work positions LUXE-NPOD in the landscape of ALP beam-dump experiments, with sensitivity comparable to FASER2 [8] and NA62 [9], and being overlapped by SHiP [10], which will have a much larger integrated luminosity. Future work will refine reconstruction algorithms and incorporate updates on the LUXE setup and experiment site, further consolidating the physics potential of LUXE-NPOD.

Acknowledgement

This research was supported by the Generalitat Valenciana (GV) via Grants CIDEGENT/2020/21 and CIPROM/2021/073; the Spanish MCIN, NextGenerationEU and GV (PRTR 2022) via Grant ASFAE/2022/015; the Spanish MCIU/AEI and European Union/FEDER via Grants PID2021-122134NB-C21 and PID2024-158190NB-C21; the CSIC via Grant 2025AEP129; the PEICTI (2021–2023) via Grant CNS2022-135420; the Alexander von Humboldt Foundation; the Estate of Dr. Moshe Glück; the Minerva Foundation with funding from the Federal Ministry of Education and Research of Germany; the Israel Science Foundation via Grants 708/20, 1235/24, and 597/24; the NSF-BSF via Grant 2021800; the Anna and Maurice Boukstein Career Development Chair; the Benoziyo Endowment Fund for the Advancement of Science; the Estate of Emile Mimran; the Estate of Betty Weneser; the Estate of Gerald Alexander; the Potter's Wheel Foundation; the Estate of Adam Glickman; the Sassoon & Marjorie Peress Legacy Fund; the Deloro Center for Space and Optics; and in part by the Krenter–Perinot Center for High-Energy Particle Physics.

I also acknowledge the computer resources at Gluon and Artemisa. Artemisa is funded by the European Union ERDF and Comunitat Valenciana as well as the technical support provided by IFIC, CSIC-UV.

References

[1] LUXE collaboration, *Eur. Phys. J. Spec. Top.* **233** (2024) 1709.

[2] LUXE collaboration, arXiv:2504.00873.

[3] Horizon Europe (2025). DOI: 10.3030/101130174.

[4] Z.Y. Bai et al., *Phys. Rev. D* **106** (2022) 115034.

[5] M. Almanza Soto et al., arXiv:2507.17716. accepted by *Phys. Rev. D*.

[6] T.G. Blackburn, B. King and S. Tang, *Phys. Plasmas* **30** (2023) 093903.

[7] A. Irles, et al. (2024). URL: https://github.com/airqui/ECALe-lcio.

[8] FASER collaboration, *Phys. Rev. D* **99** (2019) 095011.

[9] NA62 collaboration, *Eur. Phys. J. C* **85** (2025) 571.

[10] SHiP collaboration, Tech. Rep. CERN-SPSC-2023-033, SPSC-P-369.